On the Crack Spreading in Traverse Section of Bovine Bone

Longjia Li[1, 2], Tianbao Qian[2, 3] and Fei Hang[1, 2, *]

Abstract: Bone is an important natural hierarchical biomaterial which supports human body and protect organs. Its mechanical property has been researched extensively. In this experimental work, 3D microscope and scanning electron microscope (SEM) were used to research crack expansion on bovine femur cortical bone transverse section. Softwares such as image J and Photoshop were used in image and data analyses. Our results suggested that the interface energy of extending through osteons is smaller than the interface energy of extending along cement lines. Cracks are more likely to extend through osteons. Further investigations are needed to reduce errors and validate our findings.

Keywords: Crack, interface energy, toughness, SEM.

1 Introduction

We all know that bone is a human vital organ which supports human body and enable human to walk, run and lift things successfully. But like other human organs, bone can also suffer from illness such as osteoporosis and suffer physical damage such as car accident. Doing researches on bone will help human know more about bone mechanical property and fracture mechanism, so the research is good for humans. According to the author's knowledge, though there is a lot of researches on bone mechanical properties at macro scale they can't explain the toughing mechanism of bone satisfactorily. There is also a lot of researches on bone fracture process at micro scale through the method of finite element analysis and at molecular scale through the method of molecular dynamics simulation, but the simulated experiments can't get real data. Besides the simulated data obtained by computer modeling is just approximate simulation result and the experimental conclusions are less convincing. In order to enrich real experiments and basic researches, quantify the contribution of different micro cracks to bone toughness and try to explore the mechanism of bone toughening at micro scale, we decided to do this tough but meaningful work.

Bones are an anisotropic material [Gautieri, Pate, Vesentini et al. (2012); Srinivasan, Uzel, Gautieri et al. (2009); Yerramshetty, Lind and Akkus (2006)], its micro-scales

---

[1] South China University of Technology, Department of Biomedical Engineering, School of Materials Science and Engineering, Guangzhou 510000, China.

[2] National Engineering Research Center for Tissue Restoration and Reconstruction, Guangzhou 510000, China.

[3] South China University of Technology, Medical school, Guangzhou 510000, China.

*Corresponding author: F. Hang. Email: hfei@scut.edu.cn.

unique hierarchical structure [Bechtle, Ang and Schneider (2010); Buehler (2010); Dunlop and Fratzl (2010); Fang, Goldstein, Turner et al. (2012); Fratzl, Gupta, Paschalis et al. (2004); Fratzl and Weinkamer (2007); Weiner, Traub and Wagner (1999); Ziv, Wagner and Weiner (1996)] is called Haversian system [Budyn, Jonvaux and Hoc (2012); Chen, Stokes and McKittrick (2009); Conward and Samuel (2016); Lin, Xu, An et al. (2016)]. Normally the bone consists of cortical bone and cancellous bone [Blair-Levy, Watts, Fiorentino et al. (2008); Yeni, Zelman, Divine et al. (2008)], and its main components are type-I collagen and hydroxyapatite (HA) [Hulmes, Wess, Prockop et al. (1995); Wang, Li, Wei et al. (2002)]. From macro-scale considerations, temperature, loading rate [Zimmermann, Gludovatz, Schaible et al. (2014)] and ration of Ca/P have major impact on bone mechanical property. For example, Elizabeth A. Zimmermann used SAXS to do research on bone and found that bone fracture toughness became worse when the loading rate was increasing. Wen, X. X. did some experiments on ovariectomized rabbit femur cortical bone by using FTIR, DXA, Nano-indentation and Micro-CT, and found that higher ratio of Ca/P always appeared with worse cross-link of collagen [Aido, Kerschnitzki, Hoerth et al. (2015); Bousson, Meunier, Bergot et al. (2001); Daxer, Misof, Grabner et al. (1998); Green, Wang, Diab et al. (2011); Yu, Chan, Yu et al. (2014); Zhang, Gong, Zhu et al. (2015); Ziv, Wagner and Weiner (1996)]. However, the limitation of their work was that their experiments can only obtain statistical behavior of a large number of type-I collagen.

From micro-scale considerations, when human and animals are at different ages, their bone mineral distribution is also different. The different bone mineral distribution leads to different bone mechanical properties. Zhang, R's team did research on rabbit femur bone by using Micro-CT, atomic force microscopy (AFM) and scanning electron microscope (SEM), they found that the mineral content became higher at first and then became lower when the age distribution is 1 month to 17 months old, their consequence was that the age was an important variable of structural change [Zhang, Gong, Zhu et al. (2015)]. However, the limitation of the work was that it only focused on exploring the impact of composition on bone mechanical properties and it can't get the relationship between bone structure and mechanical properties.

Bone exhibits unique biocompatibility in the long-term evolution of nature [Weaver, Aizenberg, Fantner et al. (2007)]. Considering bone internal interaction at molecular level, bone toughness is affected by covalent bonds within collagen, cross-links between collagen, hydrogen bonds within and between collagen, hydrogen bonds between collagen and HA, [Buehler and Ackbarow (2007); Keten and Buehler (2008); Wei, Wang, Li et al. (2016)] and sacrificial ionic bonds [Depallea, Qina, Shefelbineb et al. (2015); Fantner, Adams, Turner et al. (2007); Fantner, Hassenkam, Kindt et al. (2005); Gautieri, Pate, Vesentini et al. (2012, 2009); Gupta, Krauss, Kerschnitzki et al. (2013); Gutsmann, Hassenkam, Cutroni et al. (2005); Hartmann and Fratzl (2009); Keten and Buehler (2008); Misof, Rapp and Fratzl (1997)]. The orientation of collagen and the collagen slippage also play important roles in bone fracture toughness [Achrai and Wagner (2013); Ger and Fratzl (2000)], took MIT's professor M. J. Buehler's work as an example, he used computer simulation to get the consequence that the hydrogen bonds within and between collagen made major contributions to bone toughness at molecular level [Buehler (2008); Chang and Buehler (2014); Chang, Flynn, Ruberty et al. (2012); Chang, Shefelbine and

Buehler (2012); Dubey and Tomar (2009); Grant, Phillips and Thomson (2012); Uzela and Buehler (2011)]. However, the limitation of the work is that the molecular dynamics simulations are just approximate simulations and the whole process can't get real data.

According to the author's knowledge, in the real experimental study on bone mechanical property, Hang Fei stretched mineralized collagen fibrils by using AFM-SEM system, he stretched out collagen fibrils from the boundary between collagen protein and non-collagen protein by using AFM probes in order to research the effects of sacrificial ionic bonds guided by Ca^{2+} on bone toughness, he got the consequence that bone micro scale and nano scale structure were the most important factors when we considered bone toughness [Hang and Barber (2011); Hang, Gupta and Barber (2014)].

The study on the bone is good for humans. But researches on bone at micro scale and nano scale is not enough, we need more in-depth researches. My work is to research cracks expansion on bovine femur bone transverse section at micro scale by using 3D microscope and SEM and then quantify its contribution to bone toughness [Cadoni, Wang, Gao et al. (2015); Goff, Lambers, Nguyen et al. (2015); Yang, van der Werf, Dijkstra et al. (2012); Zimmermann, Launey and Ritchie (2010)]. The three significances are listed below:

(1) To understand the mechanism of bone toughness better;

(2) To provide a theoretical basis for the treatment of bone diseases;

(3) To provide a theoretical basis for the design of bionic bone materials.

2 Materials and methods

2.1 Subjects

Bovine femur cortical bone was sliced by linear precision saw (IsoMet 5000, USA) to be size of 30 mm×3 mm×0.12 mm. The treatment that samples are sliced to be so thin (0.12 mm) can reduce effects of other dimensions of samples on bone mechanical property, because the larger the other dimensions were the greater probability of occurrence of micro cracks was. The 30 mm×3 mm was the size of traverse section, so we can get the information of the different cracks located at cement line and expanding through Haversian system. It was also necessary to make a notch in the middle of each sample so we can make sure that the crack expansion was initiated from the notch.

Universal materials tester (Instron 5967, Instron) was used to stretch samples to rupture. We controlled the loading rate to 0.03 mm/min and then got the instantaneous data by computer output.
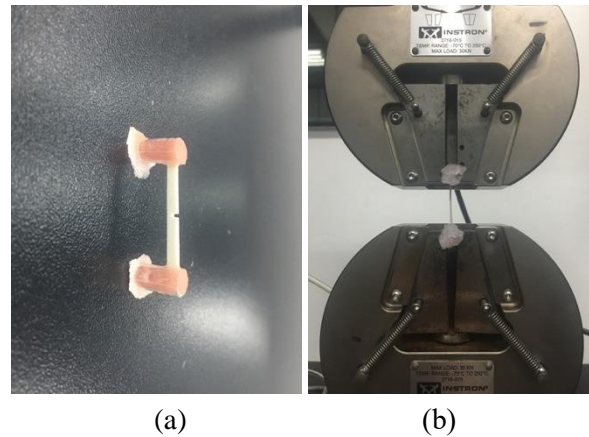
<center>(a)   (b)</center>

Figure 1: a: the treatment that the bovine femur cortical bone was sliced to be so thin (0.12 mm) can reduce the probability of occurrence of micro cracks on the section whose size was 0.12 mm×30 mm, therefore systematic errors were reduced. We also made a notch in the middle of each sample to make sure that the crack was initiated from the notch according to the principle "stress concentration". b: universal materials tester was used to stretch samples to rupture. The software of the computer connected to machine can output Stress-Strain curve and original instantaneous stress and strain data which can be used in data analyses later.

2.2 Imaging

3D microscope (HiroX7700, HiroX, Japan) was used to take picture of the fracture surface whose size was 0.12 mm×30 mm. The magnification of objective lens was 350 times and the magnification of eyepiece was 3 times, so the final magnification is 1050 times which was proved to be suitable for taking pictures. The software of 3D microscope contained the function "2D measure" which can be used to measure the widths of cracks, and the data collected can be used to calculate the interface energy of different cracks later. SEM (Merlin, Carl Zeiss AG, Germany) was used to take pictures of the fracture surface whose size was 3 mm×30 mm. We adjusted the magnification to be 40 times to get cracks' full view, and then we increased the magnification to be 160 times and took 4 pictures of each sample to get more specific information of cracks. In the picture, dark color areas stood for Haversian system and light color areas stood for inter-osteon area. JAVA program "Image J" was used to count lengths of different cracks. Then the data collected was used to be made into table and calculate the interface energy of cracks.

2.3 Image and data analysis

The software SciDavis was used to plot the Displacement-Load curve according to the data output by computer. It contained the function "Integration" which can be used to calculate the input energy (the area under the curve). Adobe Photoshop CS6 was used to splice each sample's 4 picture (the magnification was increased to 160 times) together to get full view of cracks. Because the larger the magnification of picture was the more specific information we can get, meanwhile the systematic errors were reduced.

Image J was used to count the lengths of different cracks, but first it should be set a scale

bar and the measurement process was artificial. The measurement process was one step by step by confirming the boundary, so the personal errors were unavoidable but acceptable.

Excel was used to make tables which were according to the data we collected, its function "Two-variable linear equation" also can be used to calculate different cracks' interface energy.

3 Results and disscussion

3.1 Tensile test

5 samples were stretched to rupture by universal materials tester. The data was collected by computer connected to the machine, we used Excel and SciDavis to plot according to the data. Figure 1 shows Displacement-Load curves of different samples, and that bone samples showed brittle at the loading rate of 0.03 mm/min. The different areas under curves meant different input energy which were resulted from different cracks' paths of expansion. The interface energy of different cracks was unequal, when samples broken their paths of cracks expansion contented different lengths of different cracks so the input energy was also unequal.

3.2 Pictures of samples' fracture surface taken by 3D microscope and SEM
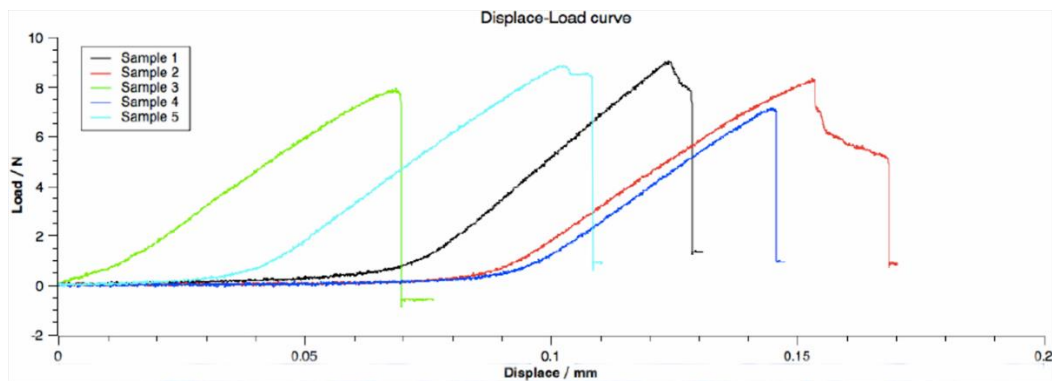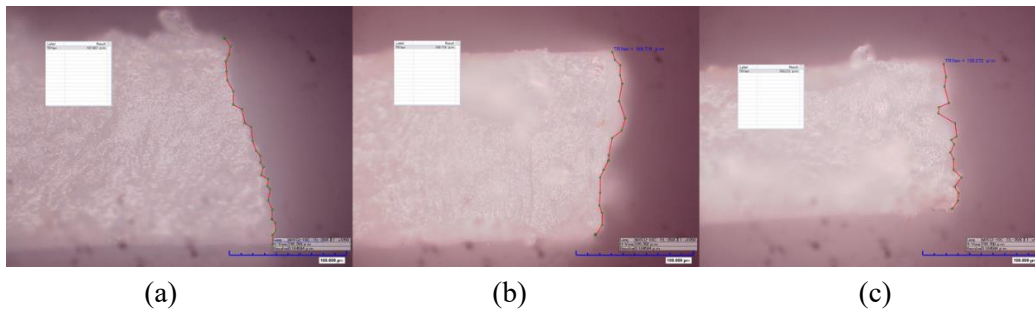

Figure 2: Displacement-Load curves of the five samples' tensile test. Instead of Stress-Strain curves we chose Displacement-Load curves because we wanted to calculate the input energy (areas under curves) directly by using software SciDavis
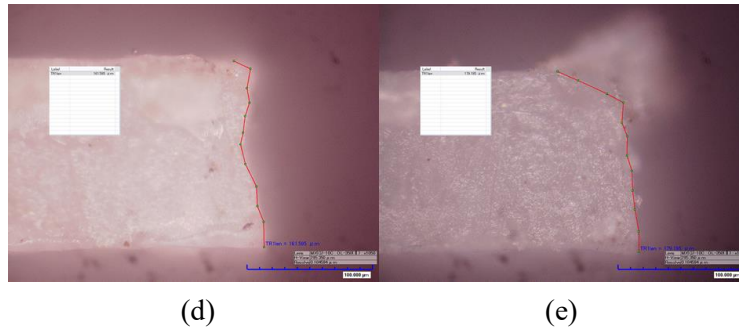

(a)   (b)   (c)

(d)   (e)

Figure 3: a, b, c, d, e were 3D microscope pictures of samples 1 to 5 and the magnification of them was 1050 times. The cracks' widths were measured by using software's function "2D measure". The data was listed in Table 1 and it can be used to calculate the different cracks' areas
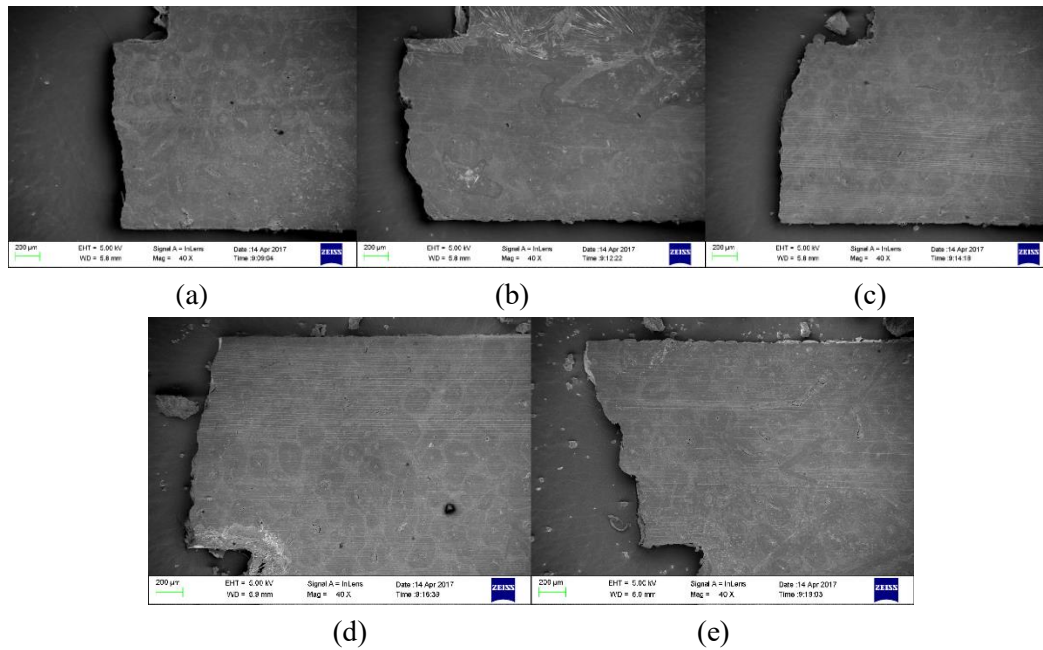

(a)   (b)   (c)

(d)   (e)

Figure 4: a, b, c, d, e were SEM pictures of samples 1 to 5 and the magnification of them was 40 times. In the Figure, Haversian system and inter-osteon area can be clearly distinguished (dark color areas stood for Haversian system and light color areas stood for inter-osteon area). We increased the magnification to be 160 times and took 4 pictures of each sample to get more detailed information
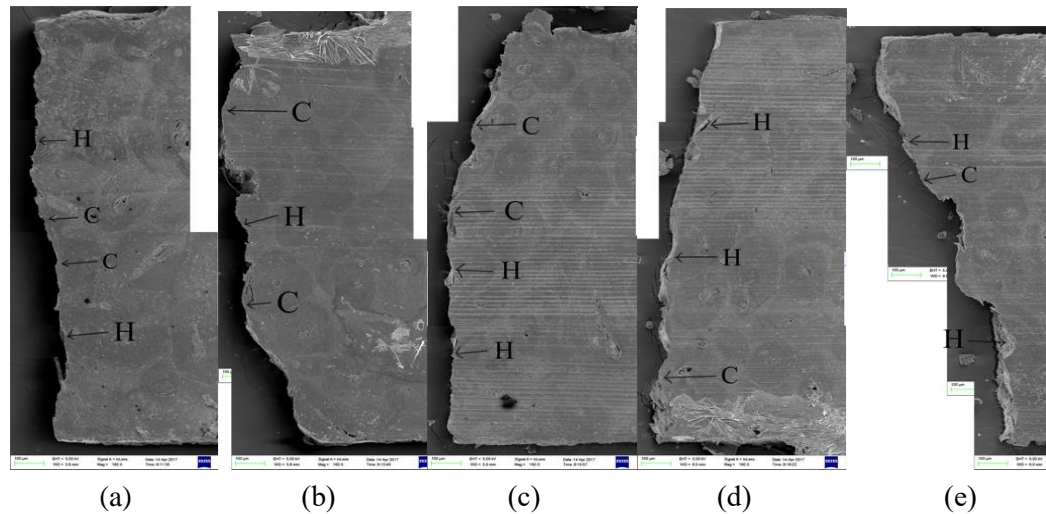
Figure 5: a, b, c, d, e were SEM pictures of samples 1 to 5 and the magnification of them was 160 times (H means Haversian system and C means cement line). We used JAVA program "Image J" to measure the lengths of different cracks. The data was listed in the Table 1 and it can be used to calculate the different cracks' areas

Figure 3 showed widths of cracks. In order to reduce errors, we sliced the sample to be so thin (0.12 mm) to make few micro cracks appear on the section whose size was 0.12 mm×30 mm. According Figure 4, SEM was also used to take pictures of cracks. Then we classified the cracks according to their paths of expansion into two kinds: the cracks extending along cement lines and the cracks extending through Haversian systems. Different paths of expansion consumed different energy. To calculate the different interface energy, we need to know the areas of different cracks. Figure 5 showed more specific SEM pictures of 5 samples whose magnification was 160 times. Adobe Photoshop CS6 was used to splice each sample's 4 pictures together, then we got full view of cracks and measured the lengths of different cracks.

3.3 Calculating the different interface energy

Table 1 listed 5 samples' cracks' widths and lengths, it also listed the input energy calculated by SciDavis according to Figure 2. It was obvious that the paths extending through osteons (Table 2 and Table 3) showed different interface energy. To get more complete information we combined every two samples' data to get ten sets of data, so we can get ten two-variable linear equations. The interface energy of cement line was set as X, the area of cement line was set as A; the interface energy of through osteons was set as Y, the area of cracks through osteons was set as B; the energy input was set as Z. Then A, B, X, Y, Z satisfied the equation:

AX+BY=Z in approximate conditions. Figure 6 (a) showed the plot according to Table 2 and Table 3. By removing the numbers that were unreasonable we got Figure 6 (b). Then Excel was used to calculate the average value of interface energy and we got the consequence: the average interface energy of cement line "X" was 2.53647 kJ/m^2, the average interface energy of through osteons "Y" was 0.78709425 kJ/m^2.

Table 1: The data was based on integration of curves in Figure 2, 3D microscope pictures in Figure 3, universal materials tester, and SEM pictures of 5 samples in Figure 5. Cracks' widths, Cracks' widths and Cracks' lengths of through osteons were listed below, H meant Haversian system and C meant cement line

Sample	1	2	3	4	5
Cracks' width μm	197.967	169.719	150.272	161.595	179.195
Length (C) μm	266.196	460.688	245.059	333.572	240.541
Length (H) μm	1464.337	1356.248	1374.417	1338.327	1585.296
Energy mm· N	0.305237	0.389725	0.268046	0.210542	0.358506

Table 2: The interface energy calculated by Excel. By combining 5 sets of data, we got 10 two-variable linear equations and we listed the solution of the equations in Table 2 and Table 3. Data combination used sample serial number in Table 1, H meant Haversian system and C meant cement line (part 1)

Data combination	1&2	1&3	1&4	1&5	2&3
Interface energy (C) kJ/m^2	4.05456	-70.2515	-1.17717	-6.95637	2.44958
Interface energy (H) kJ/m^2	0.315876	13.8237	1.126693	2.31751	0.861053

Table 3: The interface energy calculated by Excel. By combining 5 sets of data, we got 10 two-variable linear equations and we listed the solution of the equations in Table 2 and Table 3. Data combination used sample serial number in Table 1, H meant Haversian system and C meant cement line (part 2)

Data combination	2&3	2&4	2&5	3&4	3&5
Interface energy (C) kJ/m^2	7.95724	2.29377	-4.57095	1.34797	-2.95842
Interface energy (H) kJ/m^2	-1.00978	0.913978	2.11282	1.05747	1.71088

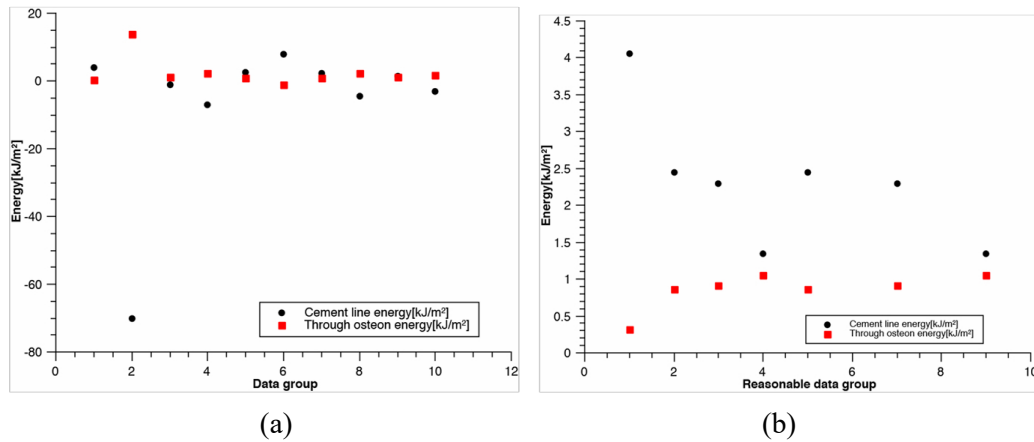(a)   (b)

Figure 6: a, b: a was plot which was according to combinations of data; b was plot that removed negative numbers and excessive numbers from Figure 6 (a). By calculating the average by Excel we got the average value of interface energy: the average interface energy of cement line was 2.53647 kJ/m^2 and the average interface energy of cracks through osteon was 0.78709425 kJ/m^2

4 Conclusion

The higher interface energy of cracks calculated was the interface energy of extending along cement lines, and the lower was the interface energy of extending through osteons, this phenomenon meant that cracks were more likely to extend through osteons for the resistance of osteons was the weaker. The lengths of extending through osteons were also the longer. At the loading rate of 0.03 mm/min the bone samples showed brittle, the phenomenon meant in the direction of bone traverse section the strain rate of 0.1% per minute made bovine femur bone show brittle. But we can still observe that the Displacement-Load curves of sample 1, sample 2 and sample 5 existed short platforms after the maximum load value. The phenomenon can be explained by mineralized collagen fibrils (MCFs) bridging: After cracks extended through samples, there are still some MCFs being not broken, the remained unbroken MCFs which acted as bridge can

connect the gaps between broken samples, therefore they need energy to make themselves completely broken so platforms appeared.

The sizes of samples varied in a wild range in Figure 3 comparing (a) and (c). The phenomenon can be resulted from systematic errors. The linear precision saw was normally used to slice macro-scale samples. Though the linear precision saw can fulfil requirements of the macro-scale sample processing it can't achieve high precision at the micro scale. In order to increase the accuracy of sample size, high-precision saw should be used in the future work.

The interface energy in the Table 2 and Table 3 appeared some unreasonable data such as negative numbers and excessive numbers, the reason may be that the contrast ratio of SEM pictures was not satisfactory which resulted in large personal errors when we measured the lengths of cracks.

The early results enriched the knowledge of bone mechanical property and bone toughing mechanism, however measures should be taken to make experiment more accurate. In order to reduce personal errors and get more accurate and convincing data, LVSEM (low voltage SEM) should be used to increase the contrast ratio of pictures in the future work. To reduce errors, more samples should also be tested. But limited manpower means that computer should be more intelligent and the experiment should be designed to be more streamlined.

Conflict of interest statement: All authors have no interest with each other neither with any department.

References

Achrai, B.; Wagner, H. D. (2013): Micro-structure and mechanical properties of the turtle carapace as a biological composite shield. *Acta Biomater*, vol. 9, no. 4, pp. 5890-5902.

Aido, M.; Kerschnitzki, M.; Hoerth, R.; Checa, S.; Spevak, L. et al. (2015): Effect of in vivo loading on bone composition varies with animal age. *Experimental Gerontology*, vol. 63, pp. 48-58.

Bechtle, S.; Ang, S. F.; Schneider, G. A. (2010): On the mechanical properties of hierarchically structured biological materials. *Biomaterials*, vol. 31, no. 25, pp. 6378-6385.

Blair-Levy, J. M.; Watts, C. E.; Fiorentino, N. M.; Dimitriadis, E. K.; Marini, J. C. et al. (2008): A type i collagen defect leads to rapidly progressive osteoarthritis in a mouse model. *Arthritis Rheum*, vol. 58, no. 4, pp. 1096-1106.

Bousson, V.; Meunier, A.; Bergot, C.; Vicaut, E.; Morais, M. H. et al. (2001): Distribution of intracortical porosity in human midfemoral cortex by age and gender. *Journal of Bone and Mineral Research*, vol. 16, pp. 1308-1317.

Budyn, É.; Jonvaux, J.; Hoc, T. (2012): Bio-morphing of progressive pathologies in haversian cortical bone. *Journal of Applied Mechanics*, vol. 79, no. 2, pp. 021001.

Buehler, M. J. (2008): Nanomechanics of collagen fibrils under varying cross-link densities: Atomistic and continuum studies. *Journal of the Mechanical Behavior of Biomedical Materials*, vol. 1, pp. 59- 67.

Buehler, M. J. (2010): Multiscale mechanics of biological and biologically inspired materials and structures. *Acta Mechanica Solida Sinica*, vol. 23, pp. 471-482.

Buehler, M. J.; Ackbarow, T. (2007): Fracture mechanics of protein materials. *Materials Today*, vol. 10, pp. 46-58.

Cadoni, E.; Wang, M.; Gao, X.; Abdel-Wahab, A.; Li, S.; Zimmermann, E. A. et al. (2015): Effect of micromorphology of cortical bone tissue on crack propagation under dynamic loading. *EPJ Web of Conferences*, vol. 94, pp. 03005.

Chang, S. W.; Buehler, M. J. (2014): Molecular biomechanics of collagen molecules. *Materials Today*, vol. 17, pp. 70-76.

Chang, S. W.; Flynn, B. P.; Ruberti, J. W.; Buehler, M. J. (2012): Molecular mechanism of force induced stabilization of collagen against en-zymatic breakdown. *Biomaterials*, vol. 33, pp. 3852-3859.

Chang, S. W.; Shefelbine, S. J.; Buehler, M. J. (2012): Structural and mechanical differences between collagen homo- and heterotrimers: Relevance for the molecular origin of brittle bone disease. *Biophysical Journal*, vol. 102, pp. 640-648.

Chen, P. Y.; Stokes, A.; McKittrick, J. (2009): Comparison of the structure and mechanical properties of bovine femur bone and antler of the north american elk (cervus elaphus canadensis). *Acta Biomaterialia*, vol. 5, pp. 693-706.

Conward, M.; Samuel, J. (2016): Machining characteristics of the haversian and plexiform components of bovine cortical bone. *Journal of the Mechanical Behavior of Biomedical Materials*, vol. 60, pp. 525-534.

Hulmes, D. J.; Wess, T. J.; Prockop, D. J.; Fratzl, P. (1995): Radial packing, order, and disorder in collagen fibrils. *Biophysical Journal*, vol. 68, pp. 1661-1670.

Daxer, A.; Misof, K.; Grabner, B.; Ettl, A.; Fratzl, P. (1998): Collagen fibrils in the human corneal stroma: Structure and aging. *Investigative Ophthalmology & Visual Science*, vol. 39, pp. 644-648.

Depallea, B.; Qina, Z.; Shefelbineb, S. J.; Buehlera, M. J. (2015): Influence of cross-link structure, density and mechanical properties in the mesoscale deformation mechanisms of collagen fibrils. *Journal of the Mechanical Behavior of Biomedical Materials*, vol. 52, pp. 1-13.

Dubey, D. K.; Tomar, V. (2009): Role of the nanoscale interfacial arrangement in mechanical strength of tropocollagen-hydroxyapatite-based hard biomaterials. *Acta Biomaterialia*, vol. 5, pp. 2704.

Dunlop, J. W.; Fratzl, P. (2010): Biological composites. *Annual Review of Materials Research*, vol. 40, pp. 1-24.

Fang, M.; Goldstein, E. L.; Turner, A. S.; Les, C. M.; Orr, B. G. et al. (2012): Type I

collagen D-spacing in fibril bundles of dermis, tendon, and bone: Bridging between nano- and micro-level tissue hierarchy. *Acs Nano*, vol. 6, pp. 9503-9514.

Fantner, G. E.; Adams, J.; Turner, P.; Thurner, P. J.; Fisher, L. W. et al. (2007): Nanoscale ion mediated networks in bone: Osteopontin can repeatedly dissipate large amounts of energy. *Nano Letters*, vol. 7, pp. 2491-2498.

Fantner, G. E.; Hassenkam, T.; Kindt, J. H.; Weaver, J. C.; Birkedal, H. et al. (2005): Sacrificial bonds and hidden length dissipate energy as mineralized fibrils separate during bone fracture. *Nature*, vol. 4, pp. 612-616.

Fratzl, P.; Gupta, H. S.; Paschalis, E. P.; Roschger, P. (2004): Structure and mechanical quality of the collagen-mineral nano-composite in bone. *The Royal Society of Chemistry*, vol. 14, pp. 2115-2123.

Fratzl, P.; Weinkamer, R. (2007): Nature's hierarchical materials. *Progress in Materials Science*, vol. 52, 1263-1334.

Gautieri, A.; Pate, M. I.; Vesentini, S.; Redaelli, A.; Buehler, M. J. (2012): Hydration and distance dependence of intermolecular shearing between collagen molecules in a model microfibril. *Journal of Biomechanics*, vol. 45, pp. 2079-2083.

Gautieri, A.; Uzel, S.; Vesentini, S.; Redaelli, A.; Buehler, M. J. (2009): Molecular and mesoscale mechanisms of osteogenesis imperfecta disease in collagen fibrils. *Biophysical Journal*, vol. 97, pp. 857-865.

Ger, I. J. P. (2000): Mineralized collagen fibrils: A mechanical model with a staggered arrangement of mineral particles. *Biophysical Journal*, vol. 79, pp. 1737-1746.

Goff, M. G.; Lambers, F. M.; Nguyen, T. M.; Sung, J.; Rimnac, C. M. et al. (2015): Fatigue-induced microdamage in cancellous bone occurs distant from resorption cavities and trabecular surfaces. *Bone*, vol. 79, pp. 8-14.

Grant, C. A.; Phillips, M. A.; Thomson, N. H. (2012): Dynamic mechanical analysis of collagen fibrils at the nanoscale. *Journal of the Mechanical Behavior of Biomedical Materials*, vol. 5, no. 1, pp. 165-170.

Green, J. O.; Wang, J.; Diab, T.; Vidakovic, B.; Guldberg, R. E. (2011): Age-related differences in the morphology of microdamage propagation in trabecular bone. *Journal of Biomechanics*, vol. 44, pp. 15, pp. 2659-2666.

Gupta, H.; Krauss, S.; Kerschnitzki, M.; Karunaratne, A.; Dunlop, J. et al. (2013): Intrafibrillar plasticity through mineral/collagen sliding is the dominant mechanism for the extreme toughness of antler bone. *Journal of the mechanical behavior of biomedical materials*, vol. 28, 366-382.

Gutsmann, T.; Hassenkam, T.; Cutroni, J. A.; Hansma, P. K. (2005): Sacri-ficial bonds in polymer brushes from rat tail tendon functioning as nanoscale velcro. *Biophysical Journal*, vol. 89, pp. 536-542.

Hang, F.; Barber, A. H. (2011): Nano-mechanical properties of individual min- eralized collagen fibrils from bone tissue. *The Royal Society*, vol. 8, 500-505.

Hang, F.; Gupta, H. S.; Barber, A. H. (2014): Nano interfacial strength between non-collagenous protein and collagen fibrils in antler bone. *Journal of the Royal Society Interface*, vol. 11.

Hartmann, M. A.; Fratzl, P. (2009): Sacrificial ionic bonds need to be randomly distributed to provide shear deformability. *Nano Letters*, vol. 9, pp. 3603-3607.

Keten, S.; Buehler, M. J. (2008): Geometric confinement governs the rupture strength of h-bond assemblies at a critical length scale. *Nano Letters*, vol. 8, pp. 743-748.

Lin, Z. X.; Xu, Z. H.; An, Y. H.; Li, X. (2016): In situ observation of fracture behavior of canine cortical bone under bending. *Mater Sci Eng C Mater Biol Appl*, vol. 62, pp. 361-367.

Misof, K.; Rapp, G.; Fratzl, P. (1997): A new molecular model for collagen elasticity based on synchrotron x-ray scattering evidence. *Biophysical Journal*, vol. 72, pp. 1376-1381.

Srinivasan, M.; Uzel, S. G.; Gautieri, A.; Keten, S.; Buehler, M. J. (2009): Al-port syndrome mutations in type iv tropocollagen alter molecular structure and nano mechanical properties. *Journal of Structural Biology*, vol. 168, pp. 503-510.

Uzela, S. G.; Buehler, M. J. (2011): Molecular structure, mechanical behavior and failure mechanism of the c-terminal cross-link domain in type I collagen. *Journal of the Mechanical Behavior of Biomedical Mateials*, vol. 4, pp. 153-161.

Wang, X.; Li, Y.; Wei, J.; Groot, K. D. (2002): Development of biomimetic nano-hydroxyapatite/poly (hexamethylene adipamide) composites. *Biomaterials*, vol. 23, pp. 4787-4791.

Weaver, J. C.; Aizenberg, J.; Fantner, G. E.; Kisailus, D.; Woesz, A. et al. (2007): Hierarchical assembly of the siliceous skeletal lattice of the hexactinellid sponge euplectella aspergillum. *Journal of Structural Biology*, vol. 158, pp. 93-106.

Wei, Q.; Wang, Y.; Li, X.; Yang, M.; Chai, W. et al. (2016): Study the bonding mechanism of binders on hydroxyapatite surface and mechanical properties for 3dp fabrication bone scaffolds. *Journal of the Mechanical Behavior of Biomedical Materials*, vol. 57, pp. 190-200.

Weiner, S.; Traub, W.; Wagner, H. D. (1999): Lamellar bone: Structure–function relations. *Journal of Structural Biology*, vol. 126, pp. 241-255.

Yang, L.; van der Werf, K. O.; Dijkstra, P. J.; Feijen, J.; Bennink, M. L. (2012): Micromechanical analysis of native and cross-linked collagen type I fibrils supports the existence of micro fibrils. *Journal of the Mechanical Behavior of Biomedical Materials*, vol. 6, pp. 148-158.

Yeni, Y. N.; Zelman, E. A.; Divine, G. W.; Kim, D. G.; Fyhrie, D. P. (2008): Trabecular shear stress amplification and variability in human vertebral cancellous bone: relationship with age, gender, spine level and trabecular architecture. *Bone*, vol. 42, no. 3, pp. 591-596.

Yerramshetty, J. S.; Lind, C.; Akkus, O. (2006): The compositional and physicochemical homogeneity of male femoral cortex increases after the sixth decade. *Bone*, vol. 39, no. 6, pp. 1236-1243.

Yu, W. S.; Chan, K. Y.; Yu, F. W. P.; Ng, B. K. W.; Lee, K. M. et al. (2014): Bone structural and mechanical indices in ado- lescent idiopathic scoliosis evaluated by high-resolution peripheral quantitative computed tomography (hr-pqct). *Bone*, vol. 61, pp. 109-115.

Zhang, R.; Gong, H.; Zhu, D.; Ma, R.; Fang, J. et al. (2015): Multi-level femoral morphology and mechanical properties of rats of different ages. *Bone*, vol. 76, pp. 76-87.

Zimmermann, E. A.; Gludovatz, B.; Schaible, E.; Busse, B.; Ritchie, R. O. (2014): Fracture resistance of human cortical bone across multiple length-scales at physiological strain rates. *Biomaterials*, vol. 35, no. 21, pp. 5472-5481.

Zimmermann, E. A.; Launey, M. E.; Ritchie, R. O. (2010): The sig- nificance of crack-resistance curves to the mixed-mode fracture toughness of human cortical bone. *Biomaterials*, vol. 31, pp. 5297-5305.

Ziv, V.; Wagner, H. D.; Weiner, S. (1996): Microstructure-micro hardness relations in parallel-fibered and lamellar bone. *Bone*, vol. 18, pp. 417.